Atmos. Chem. Phys. Discuss., 7, 16023–16053, 2007
www.atmos-chem-phys-discuss.net/7/16023/2007/

Atmospheric Chemistry and Physics Discussions

Intercomparison between aerosol optical properties by a PREDE skyradiometer and CIMEL sunphotometer over Beijing, China

H. Che[1], G. Shi[2], A. Uchiyama[3], A. Yamazaki[3], H. Chen[4], P. Goloub[5], and X. Zhang[1]

[1]Key Laboratory of Atmospheric Chemistry (LAC), Centre for Atmosphere Watch and Services (CAWAS), Chinese Academy of Meteorological Sciences (CAMS), CMA, Beijing, 100081, China
[2]State Key Laboratory of Numerical Modeling for Atmospheric Sciences and Geophysical Fluid Dynamics (LASG), Institute of Atmospheric Physics, Chinese Academy of Sciences, Beijing, 100029, China
[3]Japan Meteorological Agency, Meteorological Research Institute, 1–1 Nagamine, Tsukuba, Ibaraki 305-0052, Japan
[4]Laboratory for Middle Atmosphere and Global Environment Observation (LAGEO), Institute of Atmospheric Physics, Chinese Academy of Sciences, Beijing, 100029, China Beijing, 100029, China
[5]Laboratoire d'Optique Amosphérique, Université des Sciences et Technologies de Lille, 59655 Villeneuve d'Ascq, France

Received: 16 August 2007 – Accepted: 16 October 2007 – Published: 14 November 2007

Correspondence to: G. Shi (shigy@mail.iap.ac.cn)

Abstract

This study compares the aerosol optical and physical properties simultaneously measured by a SKYNET PREDE skyradiometer and AERONET/PHOTONS CIMEL sunphotometer at a location in Beijing, China. Aerosol optical properties (AOP) including the Aerosol Optical Depth (AOD), Angstrom exponent (α), volume size distribution, single scattering albedo (ω) and the complex refractive index were compared. The difference between the two types of instruments was less than 1.3% for the AOD and less than 4% for the single scattering albedo below the wavelength of 670 nm. There is a difference between the volume size distribution patterns derived from two instruments, which is probablely due to difference of measurement protocols and inversion algorithms for the respective instruments.

AOP under three distinct weather conditions (background, haze, and dust days) over Beijing were compared by using the retrieved skyradiometer and sunphotometer data combined with MODIS satellite results, pyranometer measurements, PM_{10} measurements, and backtrajectory analysis. The results show that the significant difference of AOP under background, haze, and dust days over Beijing is probablely due to different aerosol components under distinct weather conditions.

1 Introduction

Aerosol particles are very important in the studies of global and regional climate change (Ackerman, et al., 1981; Charlson et al., 1992) can result in direct radiative forcing as well as indirect effects on clouds (e.g. droplet properties, cloud dynamics and lifetimes) (Hansen et al., 1997). It has been speculated that aerosol particles could contribute to the global and regional dimming (Stanhill et al., 2001; Che et al., 2005) and to the change of regional precipitation (Meanon et al., 2002). Despite many aerosol studies, the aerosol concentrations and optical properties are one of the largest sources of uncertainty in current assessments and predictions of global climatic change

ACPD

7, 16023–16053, 2007

(IPCC, 2001; Hansen et al., 2000; Ramanathan et al., 2001).

To systematically study the global aerosol optical properties, the simplest and most accurate way in principle is to establish ground-based measurement networks (Holben et al., 2001). The AERONET and SKYNET are the well known two ground-based aerosol-monitoring networks which use the CIMEL CE-318 sunphotometers and PREDE skyradiotometers, respectively (Holben, 1998; Uchiyama, 2005). These two networks have been used to measure the direct and diffuse solar radiation and to derive the aerosol optical properties for the purpose of aerosol radiative forcing studies (Kim et al., 2004; Nakajima et al., 2003; Takemura et al., 2002; Dubovik et al., 2002; Eck et al., 2005; Holben et al., 2001; O'Neill et al., 2000; Smirnov et al., 2002).

Due to the difference in the measurement protocols and retrieval algorithms, it is very important to make sure that the aerosol optical properties are consistent with each other between these two networks. Though there were some intercomparison works between the results of CIMEL sunphotometer and PREDE skyradiometer (Sano et al., 2003; Campanelli et al., 2004a), it is not enough to improve the retrieval algorithms and verify the combination of the two networks.

The aim of this work is to compare nearby one year simultaneous observations of AERONET/PHOTONS and SKYNET stations in Beijing. Since the aerosol characteristics over Beijing are very representative due to heavy anthropogenic aerosol loading throughout the year and frequent dust storm events during the spring season, the comparison will shed some lights on the consistency and discrepancy of the two measurement methods and contribute to the combination of the aerosol optical properties between AERONET and SKYNET on a larger scale. This will eventually fill the gap that AERONET has in Asia.

2 Instrumentations, protocols, calibration and retrievals

2.1 Instrumentation and protocols

A PREDE POM-02 skyradiometer (SKYNET) and a CIMEL CE-318 sunphotometer (AERONET/PHOTONS) have been installed in September 2003 and March 2001, respectively at Institute of Atmospheric Physics (116.38° E, 39.97° N, 92.0 m) in Beijing, China to measure the aerosol optical properties. They have been continuously running since then. The CIMEL sunphotometer makes the direct spectral solar irradiance and sky radiance for solar almucantar scenario or principal plane scenario measurements within a 1.2° full field-of-view at five normal bands at 440, 675, 870, 940, and 1020 nm and three polarization bands at 870 nm (Holben et al., 1998). The sky-radiometer measures the solar direct irradiance and the radiance from the sky within a 1.0° full field-of-view at eleven bands of 315, 340, 380, 400, 500, 675, 870, 940, 1225, 1600, 2200 nm at every 10 or 15 min (Uchiyama et al., 2005). The sky radiance is measured at 24 pre-defined scattering angles at regular time intervals. In this study, data from five channels at 400, 500, 675, 870, and 1020 nm were used to retrieve AOP over Beijing.

A set of Kipp and Zonen CM21 pyranometer was also set up to measure the global solar irradiance (305 to 2800 nm spectral range) every 10 s automatically at Institute of Atmospheric Physics in September 2003, which is a high precision pyranometer with strictly selected domes. Because of the high optical quality of these domes the directional error is reduced to less than 10 W/m^2.

Additionally, a TEOM Series 1400a Ambient Particulate Monitor was installed at Beijing Observatory (116.47° E, 39.60° N, 31.3 m) of China Meteorological Administration (CMA) to monitor the Particle Matter (PM) mass concentration in January 2004. The instrument measured the PM_{10} mass concentrations every 5 min automatically. The mass transducer minimum detection limit is 0.01 μg. The precision for 10-m and 1-h averaged data is 5.0 $\mu g/m^3$ and 1.5 $\mu g/m^3$, respectively.

ACPD
7, 16023–16053, 2007

2.2 Calibration

The CIMEL instrument located at Beijing is calibrated using PHOTONS (http://www-loa.univ-lille1.fr/photons/) calibration facilities in Lille (LOA/USTL, France), Carpentras (Meteofrance) and Izana Observatory (INM, Spain) following the calibration protocol used by NASA staff. Accuracy on AOD is better or around 0.01 and radiance is better than 4–5% with the standard laboratory integrating sphere.

The calibration of the PREDE skyradiometer was similar to that of CIMEL sunphotometer. It was calibrated for the sky radiance using an integrating sphere at Tsukuba Space Center and for the direct solar irradiance using the Langley plot method at Mauna Loa observatory (MLO), Hawaii Island. The precision of the in situ method has been estimated to be within 1–2.5%, depending on the wavelength (Campanelli, 2004b).

2.3 Retrieval methods

Aerosol optical properties were retrieved by using Skyrad 4.2 (the latest version), which is a software to analyze the sky-radiometer data developed by Nakajima et al. (1996) and the sky radiance developed by Nakajima et al. (1996) and Dubovik and King (2000b). Measurements of CIMEL sunphotometer at 440, 675, 870, and 1020 nm are used to retrieve aerosol optical depth (Dubovik et al., 2000a). Aerosol size distribution, refractive index and single scattering albedo (ω) are retrieved by using the sky radiance almucantar measurements and the direct sun measurements (Dubovik et al., 2000b). The volume particle size distribution is retrieved in 22 logarithmically equidistant bins in the range of sizes 0.05 μm $\leq$ r $\leq$15 μm. The columnar volume spectrum is defined as:

$$\frac{dV}{d\ln r} = \frac{V_0}{\sigma\sqrt{2\pi}} \exp\left[-\frac{\left(\ln\left(r/r_m\right)\right)^2}{2\sigma^2}\right]$$

ACPD
7, 16023–16053, 2007

where dV/dlnr ($\mu m^3/\mu m^2$) is the volume distribution, V_0 is the volume concentration, and r, $r_{m,}\sigma$ denote radius, volume median radius, and standard deviation of the particles, respectively (Dubovik et al., 2002; Kim et al., 2004). The real and imaginary parts of the complex refractive index retrieved for the wavelengths corresponding to sky radiance measurements are assumed in the ranges of 1.33–1.6 and 0.0005–0.5, respectively.

Since the two radiometers are equipped with only three common wavelengths (675, 870, and 1020 nm), the optical depth at the 440 nm wavelengths for PREDE skyradiometer was calculated by using Eq. (1a) and Eq. (1b):

$$\alpha = \frac{\log_{10}\left(\frac{\tau_{400}}{\tau_{500}}\right)}{\log_{10}\left(\frac{500}{400}\right)} \quad 1(a)$$

$$\tau_{440} = \tau_{400} \cdot \left(\frac{440}{400}\right)^{-\alpha} \quad 1(b)$$

The retrieved results were compared by using the measurement data less than 3 min apart to keep relatively simultaneous observation.

3 Results and discussions

3.1 Intercomparison of AOP

The raw data retrieved by Skyrad 4.2 from the SKYNET PREDE skyradiometer were used to intercompare the level 2.0 data retrieved by the version 2 direct sun algorithm from the AERONET/PHOTONS CIMEL sunphotometer measurements which were considered as cloud-screened and high-quality data (Smirnov et al., 2000).

The intercomparisons of AOD and Angstrom exponent between the PREDE skyradiometer and CIMEL sunphotometer were based on the 3169 measurements taken within 3 min from each other for the 220 days. Figure 1 shows the plots of AOD values at each wavelength derived from the solar direct irradiance between the two instruments. High correlation was found with a significant coefficient larger than 0.995 at

each band. The difference (defined as $\frac{\text{mean}_{\text{SKYNET}} - \text{mean}_{\text{AERONET}}}{\text{mean}_{\text{AERONET}}}$%) between the two instruments at 1020 nm, 870 nm, 675 nm, and 440 nm, is less than 0.82%, 1.27%, 1.03%, and 0.91%, respectively. This confirms the high consistency of AOD for the AERONET and SKYNET measurement results.

There are significant linear correlations of Angstrom wavelength exponents computed from instantaneous measurements between the two equipments (Fig. 2). The correlation coefficient of Angstrom exponents from 440 nm to 870 nm (α_{440_870}) between two instruments is 0.84. And it is about 0.93 and 0.70 for α_{440_670} and α_{500_870}, respectively. The the linear regression equations of α_{440_870}, α_{440_670}, and α_{500_870} between the two instruments are shown in Fig. 2. The slope of α_{500_870} is only about 0.608, which is lower than those of α_{440_870} and α_{440_670}. This could be caused by no direct measurements at 500 nm for CIMEL sunphotometer. The AOD at 500 nm has to be derived from other wavelengths measurements. The whole averaged α_{440_870}, α_{440_670} and α_{500_870} based on all 3169 pairs of data between two instruments differ about 5.73%, 1.56%, and 0.06%, respectively.

Figure 3 shows the directly measured AOD results and the retrieval ones at 1020, 870, 670, and 440 nm, respectively. The directly measured AOD means the AOD was calculated from the direct solar irradiance measurement at each wavelength by using the Beer-Lambert- Bouguer law. While, the retrieved AOD means the AOD was derived from the sky radiance measurements in the almucantar plane (Nakajima et al., 1996). There are highly significant linear relationships with correlation coefficient larger than 0.999 between the measured and retrieved values for all of four wavelengths. The difference between the measured and retrieved values is about 0.35%, 0.42%, 1.23% and 0.40% for 1020, 870, 670, and 440 nm, respectively.

From the above analysis, it is seen that there is very small difference of AOD (<1.3%) and Angstrom exponent (<5.8%) for all wavelengths between PREDE Skyradiometer measurements and CIMEL sunphotometer measurements. The difference between Skyradiometer measured and retrieved values of AOD and Angstrom exponent at all wavelengths is also very small (<1.3% for AOD and <4.1% for α).

Because the daily measurements of sky radiance by CIMEL sunphotometer were less frequent than those by PREDE skyradiometer, it was found that only 142 simultaneous measurements over 69 days during all measurement period could be used to compare the single scattering albedo and the complex refractive index between two instruments. Single scattering albedo (ω) results retrieved from the skyradiometer and the sunphotometer were compared in Fig. 4. The mean values of ω retrieved from the skyradiomter are about 0.01 (1.31%), 0.03 (3.10%), 0.03 (3.40%), 0.06 (7.33%), and 0.07 (7.57%) larger than those from the sunphotometer for ω_{s400} with ω_{a440}, ω_{s400} with ω_{a500}, ω_{s670} with ω_{a670}, ω_{s870} with ω_{a870}, and ω_{s1020} with ω_{a1020}. ω_{s400} and ω_{s500} by the skyradiometer correlates to the ω_{a440} by the sunphotometer with R=0.88 and 0.86, respectively. Although the statistical analysis shows there are also obvious linear relationships (within the 99% confidence level) between the results from the skyradiometer and sunphotometer at 670, 870, and 1020 nm, their patterns are rather scattered with a correlation coefficients around 0.57, 0.45, and 0.40 respectively.

Intercomparison of the volume size distribution was carried out based on the 193 simultaneous measurements over 95 days during all the measurement period. The volumes at each bin are averaged all together for PREDE skyradiometer and CIMEL sunphotometer, respectively (Fig. 5). Generally, there is a difference between the skyradiometer and sunphotometer results. One can see that the size distribution from the sunphotometer shows a bi-mode pattern with two peak volumes at radius of 0.15 μm and 2.94 μm with the volume size spectra (dV/dlnr) of 0.07 and 0.09 $\mu m^3/\mu m^2$, while the skyradiometer shows a tri-mode pattern with three peak volume at radius of 0.17 μm and 1.69 μm and 5.29 μm with dV/dlnr of 0.06, 0.07 and 0.11 $\mu m^3/\mu m^2$, respectively. The difference between two patterns of the volume size distributions is probably due to the different retrieval algorithms. The volume size distribution from CIMEL sunphotometer measurements was retrieved by combined spherical and spheroid particle model almucantar retrievals (Dubovik, 2000b). However, there is no spheroid particle model included in Skyrad 4.2. Another possible reason is due to the data used from different channels. For the sunphotometer, four spectral channels of 440, 675, 870 and

1020 nm were used while for the skyradiometer, five spectral channels of 400, 500, 675, 870 and 1020 nm were used.

On the contrary to the single scattering albedo, the results of imaginary part of complex refractive index (m_i) retrieved from skyradiometer at all wavelengths are systemically lower than those by the sunphotometer (Fig. 6). The mean values of m_i retrieved from the skyradiometer are about 0.003, 0.006, 0.004, 0.008, and 0.008 lower than those from the sunphotometer for m_{is400} with m_{ia440}, m_{is400} with m_{ia500}, m_{is670} with m_{ia670}, m_{is870} with m_{ia870}, and m_{is1020} with m_{ia1020}, which means the AERONET results are about 1.21, 1.55, 1.83, 3.00 and 2.60 times as large as those SKYNET ones, respectively. m_{is400} and m_{is500} by the skyradiometer are linearly correlated with m_{ia440} by the sunphotometer with R=0.89 and 0.88, respectively. Although the statistical results show there are also obvious linear correlations between skyradiometer and sunphotometer at 670, 870, and 1020 nm, their correlations are also very scattered with correlation coefficients around 0.63, 0.50, and 0.49, respectively.

Generally, the difference in m_r between the two instruments is less than that in m_i (Table 1). The results for the real part of complex refractive index (m_r) show that m_r at wavelengths of 400 and 500 nm by the skyradiometer are lower than that at 440 nm by the sunphotometer but larger than that by the sunphotometer at 670, 870, and 1020 nm. The mean values of m_r retrieved from the skyradiomter are about 0.038 (2.56%), 0.036 (2.46%) lower for m_{rs400} with m_{ra440}, m_{rs400} with m_{ra500} but 0.003 (0.23%), 0.005 (0.36%), and 0.022 (1.43%) larger for m_{rs670} with m_{ra670}, m_{rs870} with m_{ra870}, and m_{rs1020} with m_{ra1020} than those from the sunphotometer

3.2 Aerosol optical properties under clean, haze and dusty days

Moderate Resolution Imaging Spectroradiometer (MODIS) satellite images (http://modis.gsfc.nasa.gov/) were used to judge the background (clean), haze (polluted) and dusty days over Beijing. From Fig. 7, it can be seen clearly that there was no pollution and cloud over Beijing on 7 September 2004 but with a heavy pollution on 13 December 2004 and sand and dust storm on 28 March 2004. To assure that no

cloud effect during the whole day, pyranometer measurement data were used to check the atmospheric status on these three days. Figure 8 presents the variation of global irradiance during the whole day on 7 September 2004 and 13 December 2004. One can see that the global solar irradiance varies very smoothly, so that we can make sure that there are not any effects of cloud on these two days. However, it was a pity that there is no pyranometer measurement on 28 March 2004.

Figure 9 presents the 5-min averages of PM_{10} concentrations on background, haze, and dusty days. From the figure one can see that the daily averaged mass concentrations are about 120, 249, and 378 $\mu g/m^3$ on the three days. On the clean day, the PM_{10} concentration varies fluctuantly before 17:00 LT (beginning of the afternoon rush hour) with an average 83 $\mu g/m^3$ and increases rapidly and varies more fluctuantly from 17:00 LT with an average ~184 $\mu g/m^3$. On the haze day, the mass concentration is as low as about 115 $\mu g/m^3$ before 09:00 LT and increases to a higher value from 09:00 LT (beginning of the morning rush hour) and varies very stably on an average of 330 $\mu g/m^3$. On the dusty day, the mass concentration is as high as about 411 $\mu g/m^3$ before 19:00 LT and decreases to a lower value from 19:00 LT and varies fluctuantly on an average of 257 $\mu g/m^3$.

Figure 10 shows the daily AOD on clean, haze and dusty days. There are 66, 42, and 8 effective measurements on these days, respectively. AOD on 7 September 2004 is very low over Beijing which could be regarded as the background AOD of Beijing. The daily averages of AOD on clean day are about 0.08±0.02, 0.07±0.02, 0.04±0.02, 0.05±0.01, 0.02±0.01 at 400, 500, 670, 870, and 1020 nm, respectively. AOD is very dependent on wavelengths during the haze day. The daily averaged AOD are about 1.20±0.10, 0.96±0.09, 0.67±0.06, 0.47±0.04, 0.39±0.03 at 400, 500, 670, 870, and 1020 nm, respectively. However, the AOD on dust day is more independent of wavelength than that on haze day. The daily averages of AOD on dust day are about 1.32±0.21, 1.27±0.19, 1.20±0.18, 1.15±0.17, 1.09±0.16 at 400, 500, 670, 870, and 1020 nm, respectively. The AOD values at 500 nm on haze day and are 13.5 and 18.0 times larger than that on clean day. These results are very similar to those from

ACPD
7, 16023–16053, 2007

AERONET measurement over Beijing (Xia et al., 2005)

The daily variation of Angstrom exponent between 440 and 870 nm under three different weather conditions are shown in Fig. 11. It varies on the range of 0.61 to 1.24, 1.33 to 1.39, and 0.15 to 0.23 on clean, haze and dust days, respectively. The averaged values of α are stably about 0.80, 1.35, and 0.20 for the clean, haze and dusty days, which clearly reflect the contributions of fine particles on haze day and coarse ones on dusty day over Beijing.

The daily variation of single scattering albedo (ω) at 400 and 500 nm under three different weather conditions are shown in Fig. 12. ω on both haze day and dusty day varies smoothly; however, SSA on the clean day fluctuates a lot. The single scattering albedo values and ranged from 0.99 to 0.78 at 400 nm and 0.99 to 0.71 at 500 nm for the clean day, 0.87 to 0.82 at 400 nm and 0.88 to 0.82 at 500 nm for the haze day, and 0.90 to 0.87 at 400 nm and 0.98 to 0.92 at 500 nm for the dusty day. The average values are about 0.90±0.08, 0.85±0.01, and 0.88±0.01 at 400 nm and 0.88±0.08, 0.86±0.01, 0.93±0.02 at 500 nm on the clean, haze and dusty days, respectively, which means the aerosol particles on haze day have more absorption ability than dusty aerosols. This can be concluded that the black carbon as well as sulfate and nitrate were the major components during haze day of Beijing. Further experiment is needed to confirm this.

Volume size distributions retrieved by PREDE skyradiometer and CIMEL sunphotometer on the clean, haze, and dusty days are shown in Fig. 13. In general, the coarse mode volumes retrieved by skyradiometer are larger than those retrieved by sunphotometer under all three distinct weather conditions. The size distributions on the clean day show the classic bi-mode patterns for both skyradiometer and sunphotometer. The effective radius of find mode is about 0.09 μm and coarse mode is about 3.48 μm for skyradiometer. It is about 0.13 μm and 2.44 μm for the fine and coarse modes from the sunphotometer. The volume size distributions on haze and dusty days both show a tri-mode patterns for skyradiometer. But a bi-mode and single mode patterns were found on haze and dusty days for sunphotometer. Although there are some difference between skyradiometer and sunphotometer retrievals on the dusty day, the fine mode

volumes with effective radii of 0.10 μm for skyradiometer and 0.15 μm for sunphotometer are very lower than the coarse mode (r_{eff}=2.38 μm for skyradiometer; r_{eff}=1.83 μm for sunphotometer) which means the large particles contributed predominately to the aerosol optical properties. While on the haze day, the fine mode volume of aerosol particles possess large scale against the total volume size distribution comparing to clean or dust days which means the fine particles contributed larger under haze day than dust day to the aerosol optical properties. The effective radii of fine mode are about 0.13 μm for skyradiometer and 0.16 μm for sunphotometer and the effective radius of coarse mode is about 2.21 μm for skyradiometer and 2.03 μm for sunphotometer.

The 5-day backtrajectory analysis on 850 hPa were calculated to examine the aerosol sources under different weather conditions by using the hybrid single-particle Lagrangian integrated trajectory (Hysplit) model of NOAA (Draxler et al., 2003). From Fig. 14, it is shown that there is a different transportation path for each atmospheric condition. The airmass on 7 September 2004 (clean day) was originally from Baikal Lake region of Siberia and past through east Mongolia southeastwardly and then acrossed North China northeastwardly to Beijing. The regions where the airmass passed were of neither pollution nor mineral dust particles. While on 13 December 2004 (haze day), the airmass was original from Shanxi Province, which is located west to Beijing with many industrial factories and coal-fired power plants with large anthropogenic aerosol emission there. It moved very slowly and passed through the west region of Hebei Province also with many industrial factories and steel plants. For the dusty days on 28 March 2004, the airmass was original from Middle Asia and stayed over Gobi Desert for a long time then moved rapidly through the desert region of North China and arrived at Beijing.

4 Conclusions

The AOD measurements between SKYNET and AERONET measurements at Beijing are highly consistent at all of four normal wavelengths with less than 1.3% differ-

ence. Angstrom coefficients differ within 10–12% between the two instruments. Single scattering albedo estimates retrieved by Skyrad 4.2 inversion are 0.03 (3.40%), 0.06 (7.33%), and 0.07 (7.57%) larger than those provided by AERONET at 670, 870 and 1020 nm. The SKYNET estimates at 400 and 500 nm are about 0.01 (1.31%), 0.03 (3.10%) larger than AERONET single scattering albedo at 440 nm with high linear relative coefficient of 0.88 and 0.86.

The volume distribution between SKYNET and AERONET are both with multi lognormal distribution patterns. On the contrary to the coarse mode, the fine mode volume concentration of SKYNET is less than that of AERONET. The size distribution retrieved from skyradiometer on the clean day shows classic bi-mode pattern with effective radius about 0.09 μm for fine mode and 3.47 μm for coarse mode. The volume size distributions retrieved from skyradiometer on haze and dust days are both shown tri-mode patterns. The effective radii are about 0.13 μm for fine mode and 2.21 μm for coarse mode under haze weather condition and about 0.10 μm for fine mode and 2.38 μm for coarse mode under dust event weather condition. The difference is probably attributed to different measurement protocols and respective inversion algorithms.

The difference of real parts of refractive index obtained using the two algorithms does not exceed 2.6%. The real parts of refractive index at wavelengths of 400 and 500 nm of skyradiometer are both lower than those of sunphotometer at 440 nm but larger than those sunphotometer values at 670, 870, and 1020 nm. The imaginary parts of refractive index of skyradiometer are less than those of sunphotometer systemically.

It is found that under the haze and dusty weather conditions, the PM_{10} is about 2 to 3 times but the AOD is about 13.7 and 18.1 times higher that that under clean conditions. AOD on the dust day is more independent of wavelength than that on haze days. The Angstrom exponents for the clean, haze and dust days are about 0.80, 1.35, and 0.20. The single scattering albedo values at 500 nm are 0.88, 0.86, 0.93 on clean, haze and dust days, respectively which indicates aerosol particles on haze day have more absorption ability than mineral aerosols on the dusty day. The five-day backtrajectory analyses show that aerosol sources under clean, haze and dust weather conditions

are originally from Baikal Lake of Siberia, regional industrial areas of western Beijing, Gobi and deserts of North China, respectively.

Although both the skyradiometer and sunphotometer used in this study have been calibrated strictly according to the manufactory's standards, differences in the retrieved AOP still exist due to the differences in the retrieval schemes. Therefore, one should consider the impact of various retrieval schemes on the AOP when they are used in radiative forcing estimates, aerosol climate impact study and satellite calibrations.

Acknowledgements. This research was financially supported by grants from National Key Project of Basic Research (2006CB403705, 2006CB403701, and 2006CB403702).

References

Ackerman, P. and Toon, O. B.: Absorption of visible radiation in atmosphere containing mixtures of absorbing and nonabsorbing particles, Appl. Opt., 20, 3661–3668, 1981.

Campanelli, M., Gobbi, G., Tomasi, C., and Nakajima, T.: Intercomparison between aerosol characteristics retrieved simultaneously with a CIMEL and PREDE sun-sky radiometers in Rome, Torvergata Aeronet site, ÓPTICA PURA Y APLICADA, 37, 3, 3159–3164, 2004 a.

Campanelli, M., Nakajima, T., and Olivieri, B.: Determination of the Solar Calibration Constant for a Sun-Sky Radiometer: Proposal of an In-Situ Procedure, Appl. Opt., 43, 651–659, 2004b.

Charlson, R. J, Schwartz, S. E., Hales, J. M., Cess, D., Coakley, J. A., and Hansen, J. E.: Climate forcing by anthropogenic aerosols, Science, 255, 423–430, 1992.

Che, H. Z., Shi, G. Y., Zhang, X. Y., Arimoto, R., Zhao, J. Q., Xu, L., Wang, B., and Chen, Z. H.: Analysis of 40 years of solar radiation data from China, 1961–2000, Geophys. Res. Lett., 32, L06803, doi:10.1029/2004GL022322, 2005.

Draxler, R. R. and Rolph, G. D.: HYSPLIT (HYbrid Single-Particle Lagrangian Integrated Trajectory) Model access via NOAA ARL READY Website (http://www.arl.noaa.gov/ready/hysplit4.html), NOAA Air Resources Laboratory, Silver Spring, MD, 2003.

Dubovik, O., Smirnov, A., Holben, B. N., King, M. D., Kaufman, Y. J., Eck ,T. F., and Slutsker, I.,: Accuracy assessments of aerosol optical properties retrieved from AERONET sun and sky radiance measurements, J. Geophys. Res., 105, 9791–9806, 2000a.

Dubovik, O. and King, M. D.: A flexible inversion algorithm for the retrieval of aerosol optical properties from Sun and sky radiance measurements, J. Geophys. Res., 105, 20 673–20 696, 2000b.

Dubovik, O., Holben, B. N., Eck, T. F., Smirnov, A., Kaufman, Y. J., King, M.D., Tanre, D., and Slutsker, I.: Variability of absorption and optical properties of key aerosol types observed in worldwide locations, J. Atm. Sci., 59, 590–608, 2002 .

Eck, T. F., Holben, B. N., Dubovik, O., Smirnov, A., Goloub, P., Chen, H. B., Chatenet, B., Gomes, L., Zhang, X. Y., Tsay, S. C., Ji, Q., Giles, D., and Slutske, I.: Columnar aerosol optical properties at AERONET sites in central eastern Asia and aerosol transport to the tropical mid-Pacific, J. Geophys. Res., 110 , D06202, doi:10.1029/2004JD005274, 2005.

Hansen, J., Sato, M., and Ruedy, R.: Radiative forcing and climate response, J. Geophys. Res., 102, 6831–6864, 1997.

Hansen, J., Sato, M., Ruedy, R., Lacis, A., and Oinas, V.: Global warming in the twenty-first century: An alternative scenario, Proc. Natl. Acad. Sci. USA, 97, 9875–9880, 2000.

Holben, B. N., Eck, T. F., Slutsker, I., et al.: AERONET – A federated instrument network and data archive for aerosol characterization, Remote Sens. Environ., 66, 1–16, 1998.

Holben, B. N., Tanre, D., Smirnov, A., et al.: An emerging ground-based aerosol climatology: Aerosol optical depth from AERONET, J. Geophys. Res., 106, 12 067–12 097, 2001.

Intergovernmental Panel on Climate Change (IPCC): Climate Change 2001: The Scientific Basis, edited by J. T. Houghton et al., 896 pp., Cambridge Univ. Press, New York, 2001.

Kim, D. H., Sohn, B. J., Nakajima, T., Takamura, T., Choi, B. C., and Yoon, S. C.: Aerosol optical properties over east Asia determined from ground-based sky radiation measurements, J. Geophys. Res., 109, D02209, doi:10.1029/2003JD003387, 2004.

Menon, S., Hansen, J. E., Nazarenko, L., and Luo, Y. F.: Climate effects of black carbon aerosols in China and India, Science, 297, 2249–2252, 2002.

Nakajima, T., Sekiguchi, M., Takemura, T., et al.: Significance of direct and indirect radiative forcings of aerosols in the East China Sea region, J. Geophys. Res., 108, 8658, doi:10.1029/2002JD003261, 2003.

Nakajima, T., Tonna, G., Rao, R., and Holben, B. N.: Use of sky brightness measurements from ground for remote sensing of particulate polydispersions, Appl. Opt., 35, 2672–2686, 1996.

O'Neill, N. T., Ignatov, A., Holben, B. N., and Eck, T. F.: The lognormal distribution as a reference for reporting aerosol optical depth statistics; Empirical tests using multi-year, multi-site AERONET sunphotometer data, J. Geophys. Lett., 27, 20, 3333–3336, 2000.

Ramanathan, V., Crutzen, P. J., Lelieveld, J., et al.: The Indian Ocean Experiment: An integrated analysis of the climate forcing and effects of the great Indo-Asian haze, J. Geophys. Res., 106, 28 371–28 398, 2001.

Sano, I., Mukai, S., Yamano, M., Takamura, T., Nakajima, T., and Holben, B. N.: Calibration and validation of retrieved aerosol properties based on Aeronet and Skynet, Adv. Space Res., 32, 11, 2159–2164, 2003.

Smirnov, A., Holben, B. N., Eck, T. F., Dubovik, O., and Slutsker, I.: Cloud screening and quality control algorithms for the AERONET database, Rem. Sens. Env., 73, 337–349, 2000.

Smirnov, A., Holben, B. N., Eck, T. F., Slutsker, I., Chatenet, B., and Pinker, R. T.: Diurnal variability of aerosol optical depth observed at AERONET (Aerosol Robotic Network) sites, Geophys. Res. Lett., 29, 23, 2115, doi:10.1029/2002GL016305, 2002.

Stanhill, G. and Cohen, S.: Global dimming: a review of the evidence for a widespread and significant reduction in global radiation with discussion of its probable causes and possible agricultural consequences, Agr. Forest Meteorol., 107, 255–278, 2001.

Takemura, T., Nakajima, T., Dubovik, O., Holben, B. N., and Kinne, S.: Single scattering albedo and radiative forcing of various aerosol species with a global three-dimensional model, J. Climate, 15, 333–352, 2002.

Uchiyama, A., Yamazaki, A., Togawa, H., and Asano, J.: Characteristics of Aeolian dust observed by sky-radiometer in the Intensive Observation Period 1 (IOP1), J. Meteor. Soc. Japan, 83A, 291305, 2005.

Xia, X. A., Chen, H. B., Wang, P. C., Zong, X. M., Qiu, J. H., and Goloub, P.: Aerosol properties and their spatial and temporal variations over North China in spring 2001, Tellus, 57B, 28–39, 2005.

Table 1. Averaged single scattering albedo, refractive index, and their absolute and percentage differences between skyradiometer and sunphotometer at all wavelengths for all simultaneous data.

	440/400 nm	440/500 nm	670 nm	870 nm	1020 nm
ω_a	0.88	0.88	0.89	0.87	0.86
ω_s	0.89	0.90	0.93	0.94	0.93
m_{ra}	1.48	1.48	1.50	1.51	1.52
m_{rs}	1.51	1.51	1.50	1.51	1.49
m_{ia}	0.017	0.017	0.011	0.012	0.013
m_{is}	0.014	0.011	0.006	0.004	0.005
$\delta\omega$	−0.01	−0.03	−0.03	−0.06	−0.07
δm_r	−0.04	−0.04	0.00	0.01	0.02
δm_i	0.003	0.006	0.004	0.008	0.008
$\delta\omega$%	−1.31	−3.10	−3.40	−7.33	−7.57
δm_r %	−2.56	−2.46	0.23	0.36	1.43
R_{mi}	1.21	1.55	1.83	3.00	2.60

ω, m_r and m_i mean averaged single scattering albedo, real part of refractive index and the imaginary part of refractive index; subscript a and s means AERONET sunphotometer and SKYNET skyradiometer; δ- and δ-% mean absolute and percentage difference between skyradiometer and sunphotometer, respectively. R_{mi} means the ratio of AERONET m_i to SKYNET m_i.

ACPD
7, 16023–16053, 2007

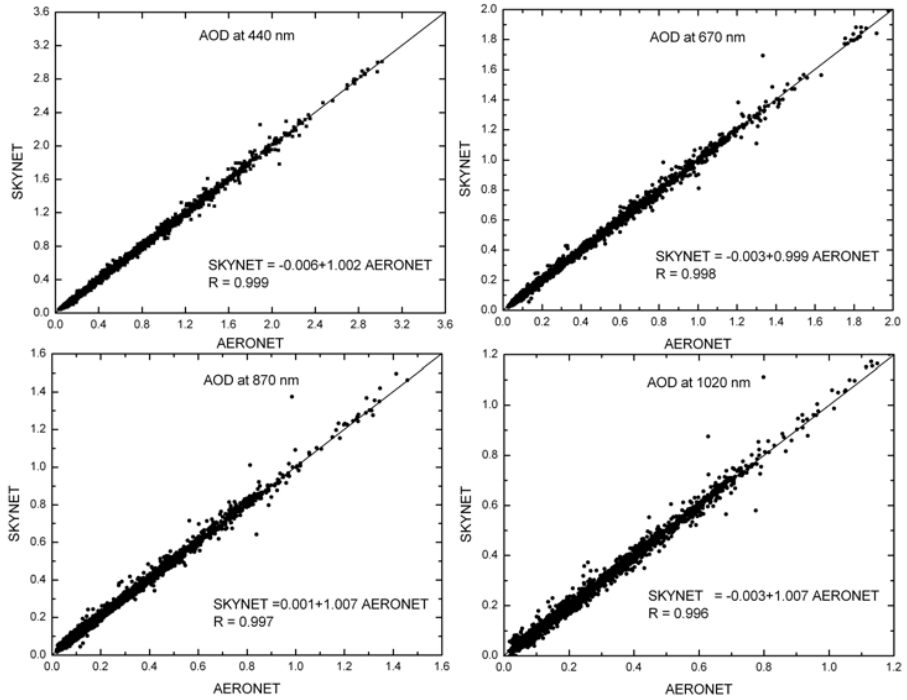

Fig. 1. Scattergrams of aerosol optical depth between PREDE skyradiometer and CIMEL sunphotometer data at wavelengths of 440, 670, 870 and 1020 nm over Beijing.

ACPD
7, 16023–16053, 2007

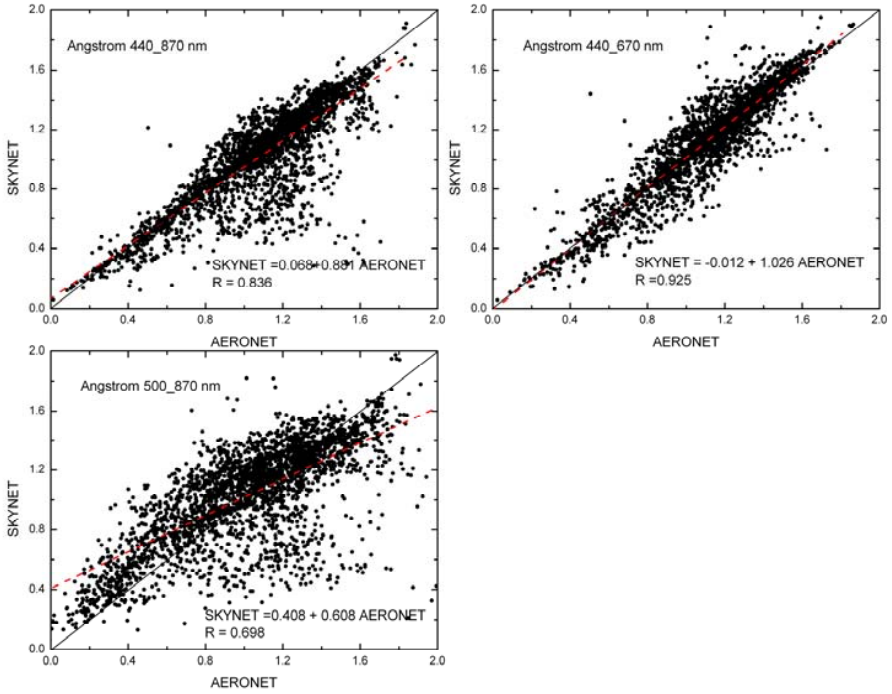

Fig. 2. Scattergrams of Angstrom exponent at 440–870 nm, 440–670 nm, and 500–870 nm between PREDE skyradiometer and CIMEL sunphotometer data over Beijing.

ACPD
7, 16023–16053, 2007

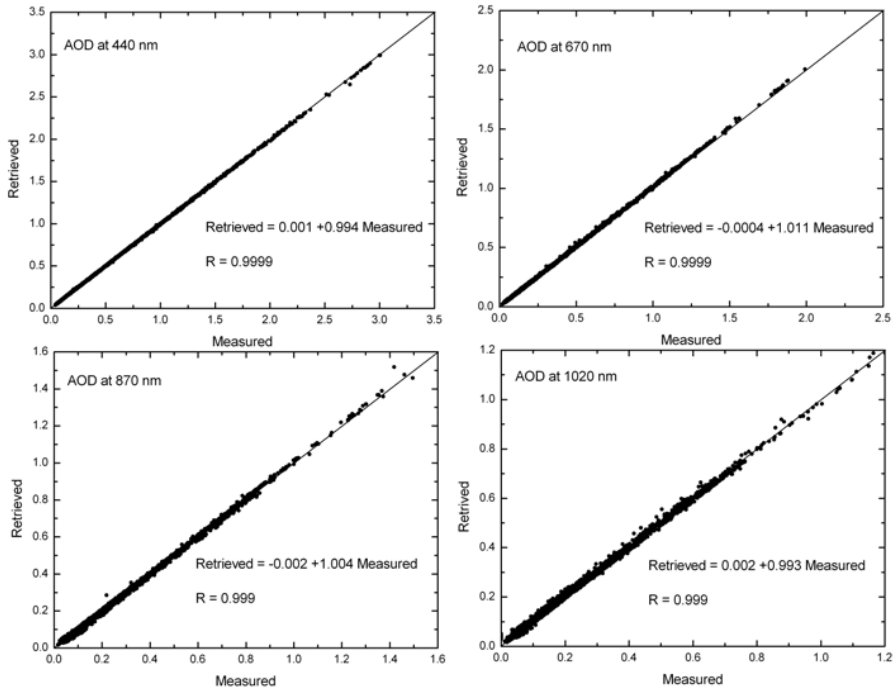

Fig. 3. Scattergrams of aerosol optical depth between the retrieved and measured results of skyradiometer over Beijing.

ACPD
7, 16023–16053, 2007

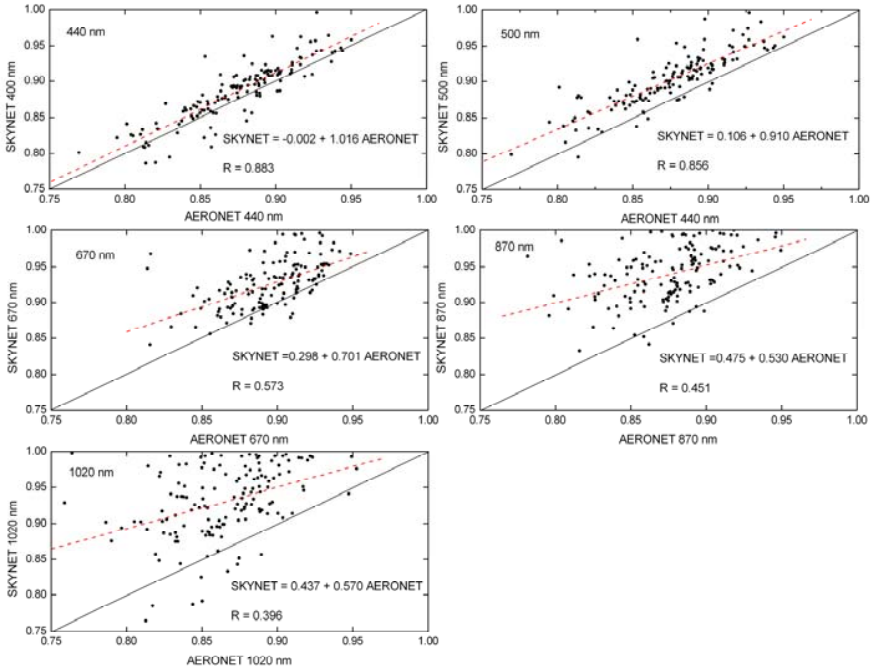

Fig. 4. Scattergrams of single scattering albedo between PREDE skyradiometer and CIMEL sunphotometer data at wavelengths of 400, 500, 670, 870 and 1020 nm over Beijing.

ACPD
7, 16023–16053, 2007

EGU

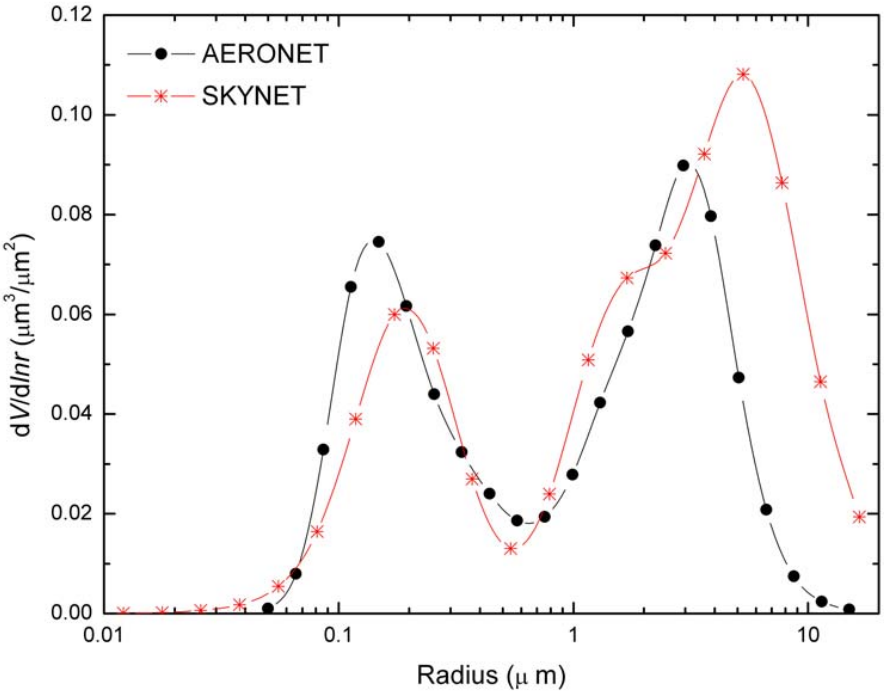

Fig. 5. Retrieved volume size distribution of PREDE skyradiometer and CIMEL sunphotometer over Beijing.

ACPD
7, 16023–16053, 2007

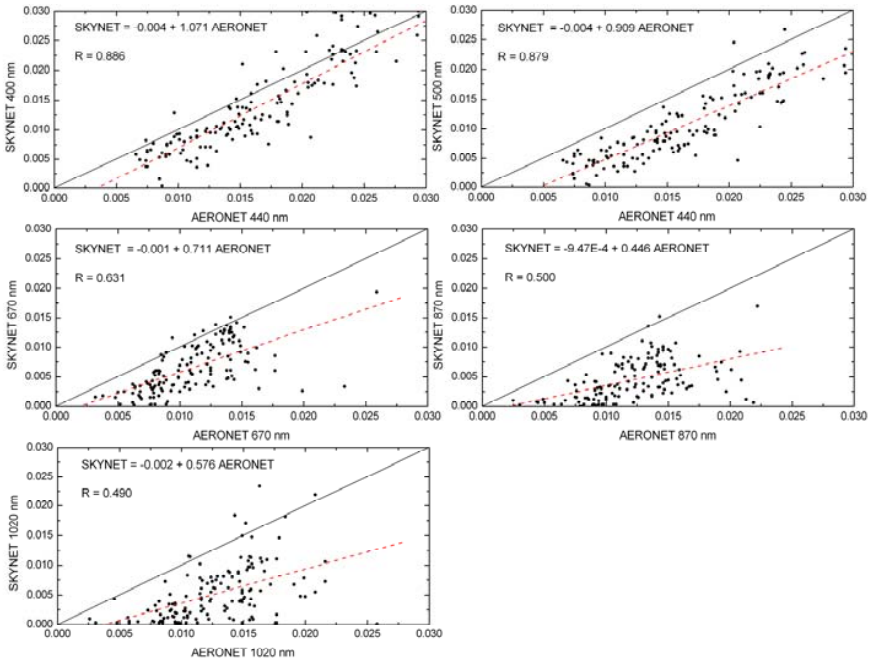

Fig. 6. Scattergrams of imaginary part of refractive index between PREDE skyradiometer and CIMEL sunphotometer data at wavelengths of 400, 500, 670, 870 and 1020 nm over Beijing.

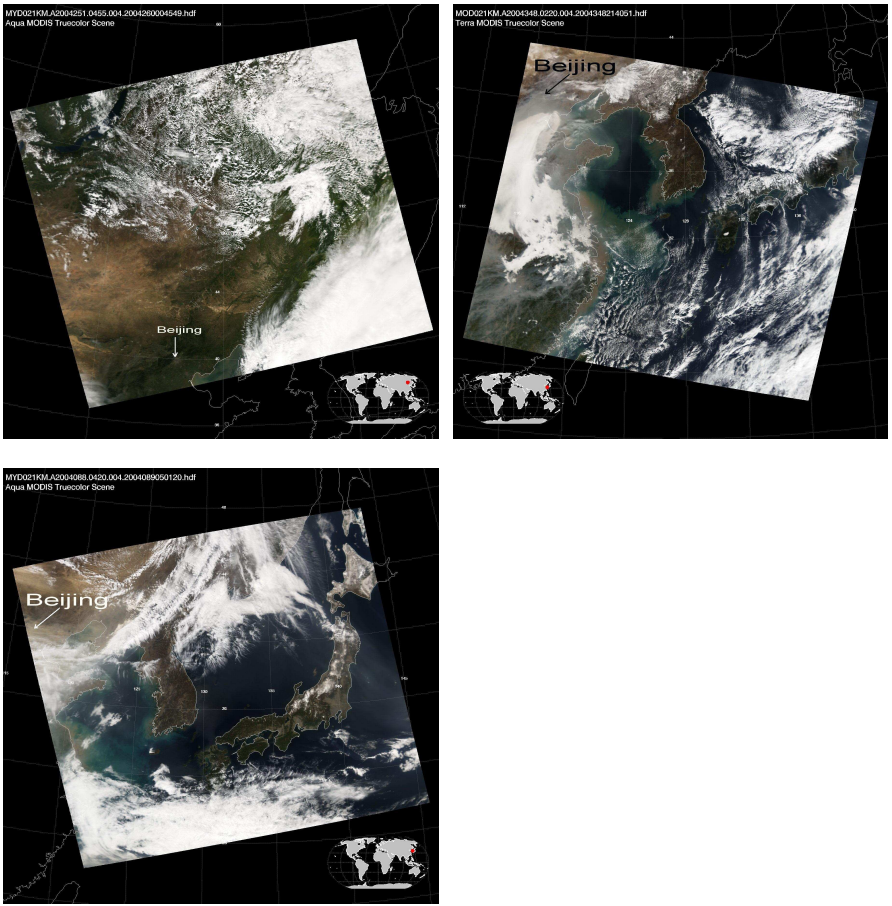

Fig. 7. MODIS images under clean (top-left), haze (top-right) and dust (bottom-left) weather conditions over Beijing on 7 September 2004, 13 December 2004, and 28 March in 2004.

ACPD
7, 16023–16053, 2007

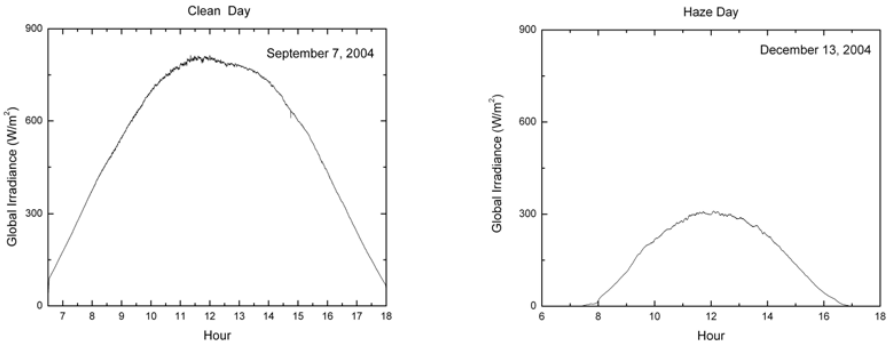

Fig. 8. 10-s averages of global solar irradiance of Kipp and Zonen CM21 pyranometer measurement under clean (left) and haze (right) weather conditions over Beijing on 7 September 2004, 13 December in 2004.

ACPD
7, 16023–16053, 2007

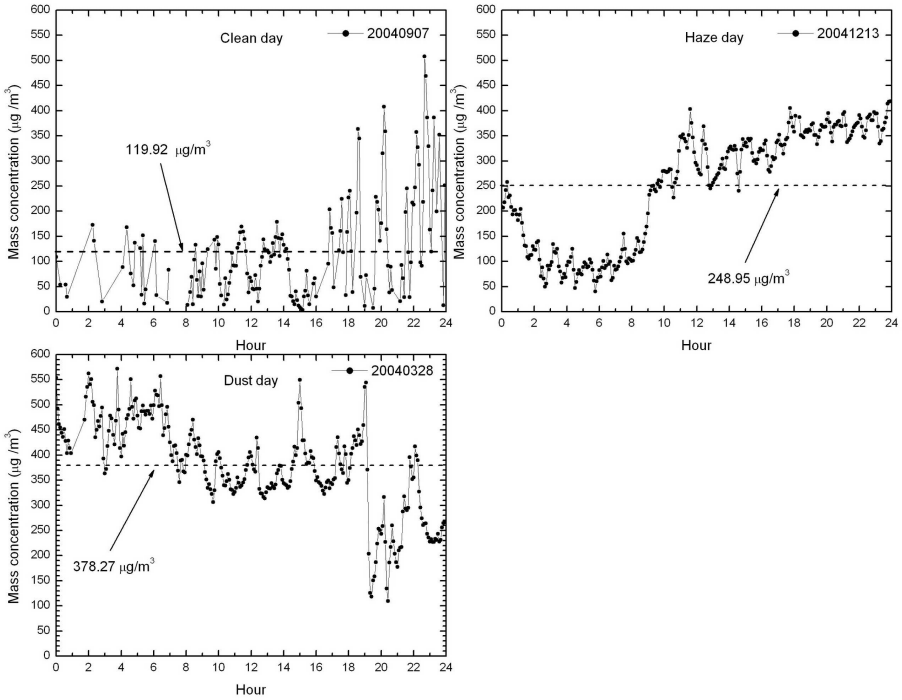

Fig. 9. Five-minute averages of PM_{10} concentration under clean (top-left), haze (top-right) and dust (bottom-left) weather conditions over Beijing on 7 September 2004, 13 December 2004, and 28 March in 2004.

ACPD
7, 16023–16053, 2007

EGU

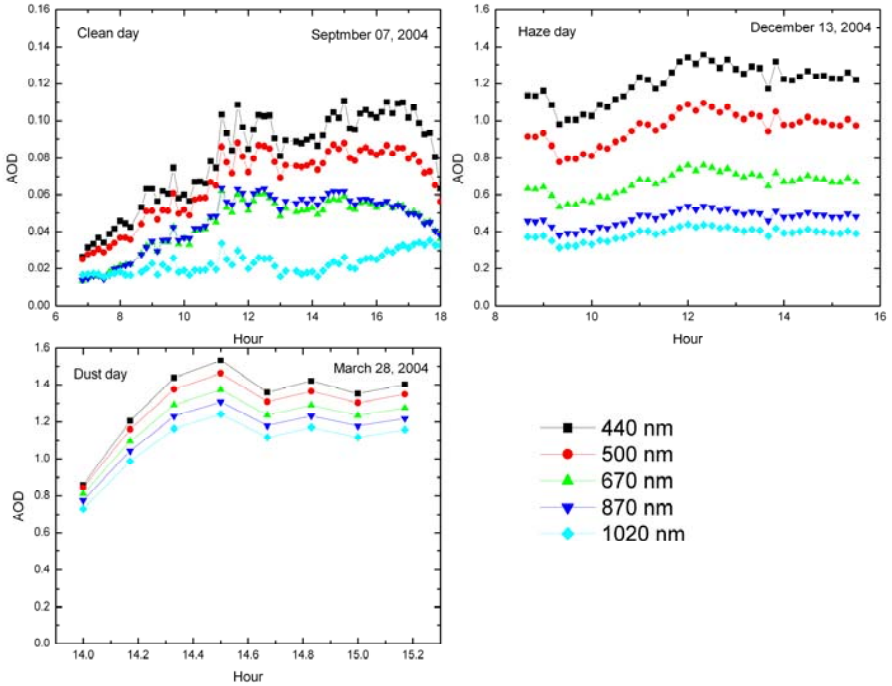

Fig. 10. AOD at 440, 500, 670, 870, and 1020 nm from directly-measured skyradiometer data under clean (top-left), haze (top-right) and dust (bottom-left) weather conditions over Beijing on 7 September 2004, 13 December 2004, and 28 March in 2004.

ACPD
7, 16023–16053, 2007

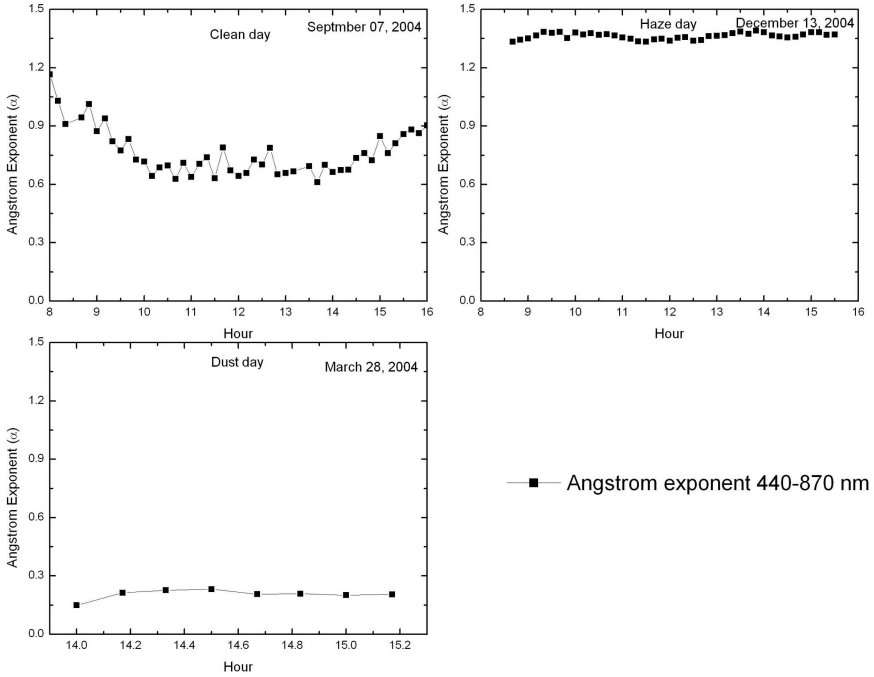

Fig. 11. Angstrom exponent (α) at 440–870 nm of skyradiometer under clean (top-left), haze (top-right) and dust (bottom-left) weather conditions over Beijing on 7 September 2004, 13 December 2004, and 28 March in 2004.

ACPD
7, 16023–16053, 2007

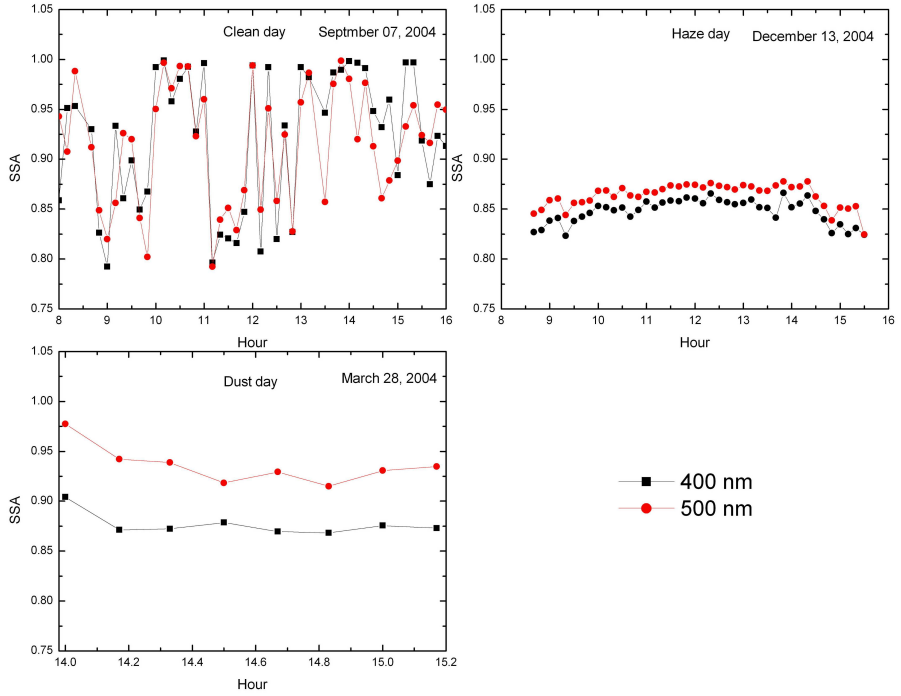

Fig. 12. Single scattering albedo (ω) at 400 and 500 nm retrieved from skyradiometer data under clean (top-left), haze (top-right) and dust (bottom-left) weather conditions over Beijing on 7 September 2004, 13 December 2004, and 28 March in 2004.

ACPD
7, 16023–16053, 2007

EGU

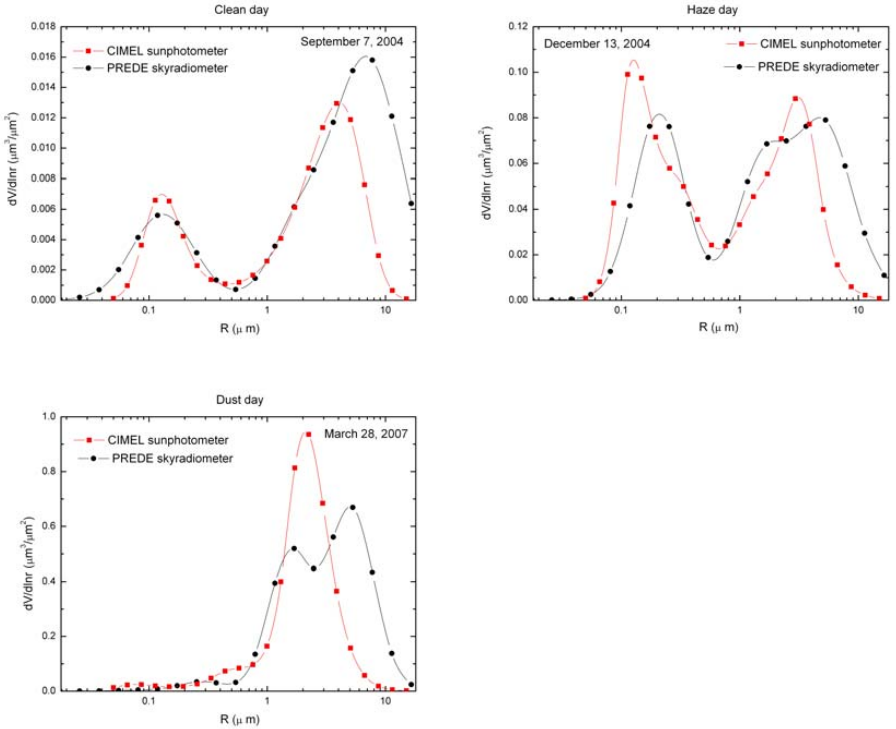

Fig. 13. Volume size distributions retrieved from skyradiometer and sunphotometer data under clean (top-left), haze (top-right) and dust (bottom-left) weather conditions over Beijing on 7 September 2004, 13 December 2004, and 28 March in 2004.

ACPD
7, 16023–16053, 2007

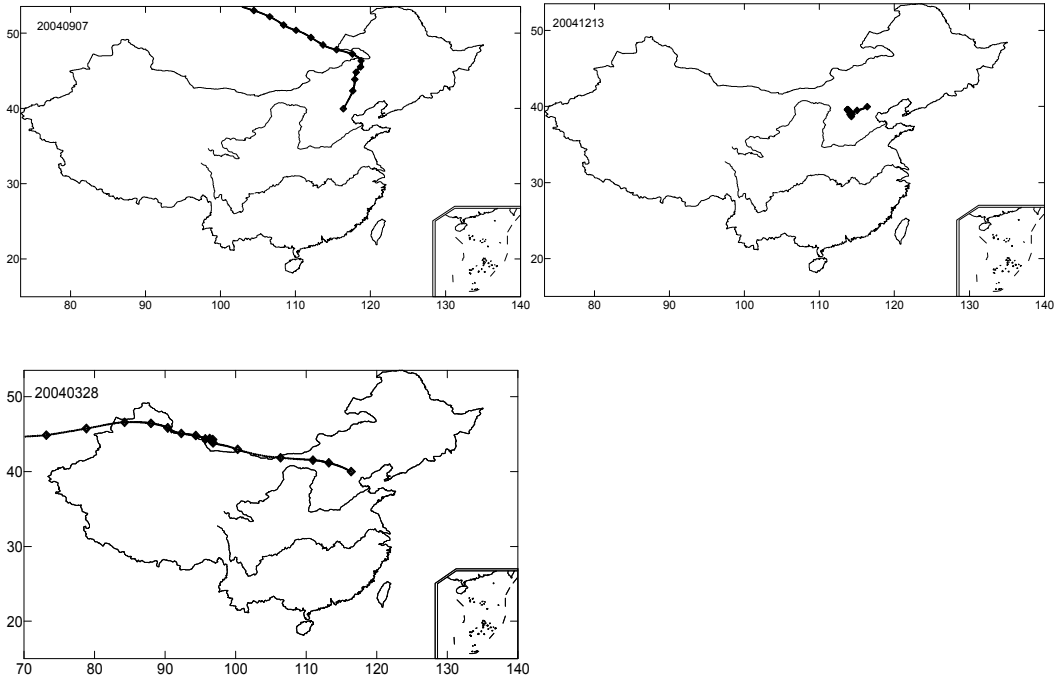

Fig. 14. The five day backtrajectory analyses under clean (top-left), haze (top-right) and dust (bottom-left) weather conditions over Beijing on 7 September 2004, 13 December 2004, and 28 March in 2004.

ACPD
7, 16023–16053, 2007